

Femtosecond spontaneous-emission studies of reaction centers from photosynthetic bacteria

(electron transfer/*Rhodobacter sphaeroides*/*Rhodobacter capsulatus*)

MEI DU^{†‡}, SANDRA J. ROSENTHAL^{†‡}, XIAOLIANG XIE^{†§}, THEODORE J. DiMAGNO^{†¶}, MARK SCHMIDT^{†‡},
DEBORAH K. HANSON^{**}, MARIANNE SCHIFFER^{**}, JAMES R. NORRIS^{†||}, AND GRAHAM R. FLEMING^{†‡}

[†]Department of Chemistry, and [‡]The James Franck Institute, The University of Chicago, Chicago, IL 60637; and [¶]Chemistry Division and ^{**}Biological and Medical Research Division, Argonne National Laboratory, Argonne, IL 60439

Communicated by R. Stephen Berry, May 29, 1992

ABSTRACT Spontaneous emission from reaction centers of photosynthetic bacteria has been recorded with a time resolution of 50 fs. Excitation was made directly into both the special-pair band (850 nm) and the Q_x band of bacteriochlorophylls (608 nm). *Rhodobacter sphaeroides* R26, *Rhodobacter capsulatus* wild type, and four mutants of *Rb. capsulatus* were studied. In all cases the fluorescence decay was not single exponential and was well fit as a sum of two exponential decay components. The short components are in excellent agreement with the single component detected by measurements of stimulated emission. The origin of the nonexponential decay is discussed in terms of heterogeneity, the kinetic scheme, and the possibility of slow vibrational relaxation.

The mechanism of the initial electron transfer step in the reaction center (RC) of photosynthetic bacteria has been the subject of intense study over the past 10 years. This initial step is ultrafast, occurring in about 3 ps at room temperature (1). As the understanding of the RC improves the need arises for more precise kinetic data. In particular, questions arise as to the exponentiality of the observed kinetic signals (2–8), the possibility of differing behavior at different wavelengths (3, 4), the existence of oscillatory components (5), and the existence of spectral shifts (3, 6) accompanying the excitation and subsequent electron transfer processes.

The primary method used for ultrafast studies of the primary charge separation step has been time-resolved absorption spectroscopy, generally with low-repetition-rate (10–30 Hz) relatively high-power (excitation pulse energies in the range 1–30 μ J) laser systems. In addition to the limited dynamic range and signal/noise ratios of such measurements, precise determination of kinetics requires that accurate account be taken of all the competing absorptions and bleachings at the detection wavelength. In measurements of the decay of the excited state of the special pair (P^{*}) by stimulated emission, most workers have made measurements at or near the isosbestic point in the spectrum consisting of ground state (P) bleaching and absorption of the radical cation of P (P⁺) and P^{*}. However, such a procedure makes it difficult to observe longer decay components in the stimulated emission and to look for the presence of spectral evolution or wavelength-dependent kinetics. Zinth and coworkers (7) could not rule out the presence of a 10- to 20-ps component within their experimental accuracy. More recently Vos *et al.* (5), after significantly improving their signal/noise ratio, reported that the stimulated emission in *Rhodobacter sphaeroides* R26 (R26) did not decay exponentially but was well described by two decay times (2.9 and 12 ps) with relative amplitudes of 65% and 35%. This observation is very significant for kinetic

analyses of absorption changes in other portions of the spectrum, in particular for discussion of whether the primary process should be described by a one-step superexchange or two-step sequential mechanism (2–15).

An alternative to time-resolved absorption spectroscopy is to measure the spontaneous emission from P^{*} with appropriate time resolution. In this case the long time value of the signal amplitude is clearly defined and studies as a function of detection wavelength are relatively straightforward. We have developed a reflective optics upconversion system that is particularly suited for fluorescence studies using low-energy (≈ 1 nJ), high-repetition-rate excitation sources. Here we describe spontaneous-emission studies of RCs obtained with a time resolution of ≈ 50 fs for R26, *Rhodobacter capsulatus*, and several mutants of *Rb. capsulatus* in which amino acids in the M208 or L181 positions have been modified.

EXPERIMENTAL PROCEDURES

R26 samples and *Rb. capsulatus* mutants were prepared as described (16, 17). For all samples Q_A was chemically reduced with the exception of one, the R26 sample in which Q_A was removed (18, 19). All measurements were carried out at room temperature. The samples had an optical density of 0.5 at 608 nm or 0.8 at 850 nm in a 1-mm-optical-pathlength cell and were stirred during the course of an experiment. Fluorescence intensity at time zero did not change during consecutive scans. The absorption spectrum of the sample was recorded before and after each measurement. Only the R26 Q_A-removed sample in the 850-nm experiments showed signs of deterioration.

Two different laser systems were used. Excitation at 850 nm was provided by a Mira 900 F titanium sapphire laser (Coherent, Palo Alto, CA). Typical output pulses were 90 fs long, 6 nJ per pulse, and the repetition rate was 80 MHz. The sample was excited with ≈ 1 -nJ pulses, while the gate pulse was ≈ 2 nJ. Excitation at 608 nm was provided by a cavity-dumped, anti-resonant ring dye laser amplified in a two-stage single-pass dye amplifier pumped by the frequency-doubled output of a neodymium:yttrium aluminum garnet regenerative amplifier operating at 100-kHz repetition rate (20). This system typically yielded 60-fs pulses of 240 nJ. The sample was excited with 3- to 4-nJ pulses and the gate pulse was typically 7–8 nJ.

The fluorescence upconversion spectrometers used with the two laser systems were essentially identical and are described in detail elsewhere (21). In brief, the gate pulse traverses a variable delay before being combined with the

Table 1. Best fits at 850-nm excitation, 940-nm emission

RC	a_1 , %	τ_1 , ps	a_2 , %	τ_2 , ps
R26				
Q _A reduced	80.8 ^{69.1} _{5.6}	2.7 ^{2.2} _{3.2}	19.2 ^{30.9} _{14.1}	12.1 ^{18.5} _{21.0}
Q _A removed	84.1 ^{55.0} _{19.4}	3.0 ^{1.9} _{4.3}	15.9 ^{48.7} _{33.7}	19.8 ^{7.0} _{50.0}
Rb. capsulatus				
Wild type	72.3 ^{49.7} _{30.5}	2.7 ^{1.7} _{3.7}	27.7 ^{50.0} _{7.8}	11.1 ^{17.8} _{49.3}
Phe L181 → Tyr	84.4 ^{50.6} _{19.1}	2.3 ^{1.6} _{3.0}	15.6 ^{38.8} _{7.1}	10.5 ^{5.4} _{29.0}
Tyr L181,				
Phe M208	59.5 ^{44.0} _{14.4}	3.5 ^{2.0} _{5.2}	40.5 ^{55.7} _{13.9}	24.2 ^{15.9} _{30.0}
Tyr M208 → Phe	53.3 ^{40.8} _{16.7}	5.4 ^{3.2} _{9.0}	46.7 ^{58.8} _{30.1}	40.0 ^{29.0} ₁₁₅

Standard deviations were determined by fixing the parameter of interest and allowing all other variables to float. The fixed parameter was increased and decreased until the reduced χ^2 of the fit had increased an amount corresponding to one standard normal deviate (22, 23).

sample fluorescence in a 0.4-mm (608-nm system) or 0.5-mm (850-nm system) LiIO₃ crystal while the excitation pulse traverses a fixed delay before being focused into a 1-mm-pathlength sample cell positioned at one of the foci of an elliptical reflector. The LiIO₃ crystal is positioned at the other focus of the reflector and the sum frequency of the fluorescence and gate pulse is directed into a double monochromator and detected by photon counting. Autocorrelation of the excitation and gate pulse yielded an instrument response function of ≈ 160 fs (full width at half-maximum) (850-nm experiments) and ≈ 70 fs (608-nm experiments). In the 608-nm studies fluorescence was collected at the magic angle, while in the 850-nm studies the fluorescence component parallel to the excitation polarization was collected.

RESULTS

Fluorescence decays could not be fit as single exponential or stretched exponential and were well fit to double exponential decays convoluted with an instrument response function, plus a flat background. The parameters obtained from fits of the spontaneous emission decays recorded with 850-nm excitation are tabulated in Table 1. A typical data set and fit are shown in Fig. 1. All the samples showed nonexponential decay with a major short component corresponding well to our previous stimulated-emission measurements (24) and a longer component in the range 10–70 ps being present in all samples. Examining the R26 data, we note little difference was observed between samples in which Q_A was reduced or removed. This finding was also confirmed by stimulated emission measurements carried out at 20-Hz repetition rate (pump, 860 nm; probe, 925 nm (C.-K. Chan, T.J.D., J.R.N., and G.R.F., unpublished data)).

Turning to the *Rb. capsulatus* mutants, we note that the Phe L181 → Tyr mutant gives a more rapid short component than wild type, as was observed in stimulated emission (24). The short component is identical within error to the single component determined from stimulated-emission measurements for the wild type and the Phe L181 → Tyr and Phe L181 → Tyr, Tyr M208 → Phe mutants. However, the short

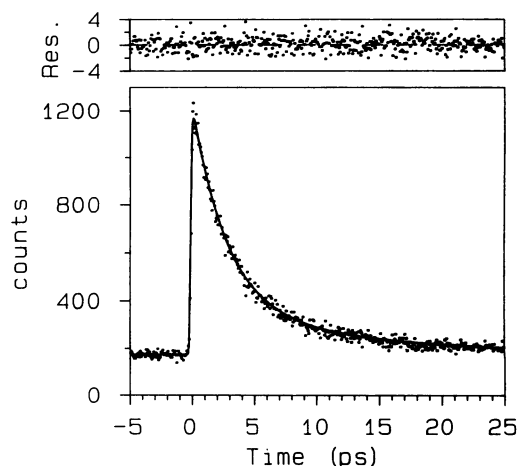


FIG. 1. Spontaneous emission decay of P* in *Rb. sphaeroides* R26 with excitation at 850 nm and emission at 940 nm. Solid line is a double exponential fit with $a_1 = 80.8\%$, $\tau_1 = 2.7$ ps, $a_2 = 19.2\%$, and $\tau_2 = 12.1$ ps. Res., residual.

component for the Tyr M208 → Phe mutant, 5.4 ps, is shorter than that obtained previously [9.2 ps (24)]. Viewing the whole data set, we find that as the short component slows, both decay time and amplitude of the longer component increase.

Table 2 lists fitting results obtained for 608-nm excitation of R26 with Q_A removed and *Rb. capsulatus* Tyr M208 → Thr mutant. Fig. 2 shows a typical data set. The short and long decay components are within error the same as determined with 850-nm excitation. The decay of the R26 with Q_A in its normal state is within error the same as for R26 with Q_A removed. The Tyr M208 → Thr mutant gives a shorter fast component, 10.0 ps, than obtained previously [15 ps (24)]. However, in the 608-nm data with adequate signal/noise we find a rise time of 150–250 fs. Fig. 3 compares data detected at 940 nm for both excitation wavelengths. Attempts to observe a rise time at 940 nm and 960 nm with 850-nm excitation were unsuccessful and we conclude that such a rise time, if it exists and has an amplitude equal to that of the short decay component, is <20 fs when P is directly excited. A complexity in the 608-nm experiments is the group velocity mismatch between the 880- to 940-nm fluorescence and the 608-nm gate pulse. We calculate the group velocity mismatch in our 0.4-mm LiIO₃ crystal to be 115–130 fs for this wavelength range (25). Thus the group velocity mismatch adds 115–130 fs to the instrument response function, yielding a total width of 185–200 fs. However, the instrument function would have to be ≈ 350 fs wide to obscure the 200-fs rise time, and we conclude that the rise time is not an artifact of the group velocity mismatch.

DISCUSSION

With the exception of very recent work by Vos *et al.* (5) previous studies of the decay of stimulated emission from bacterial RCs have reported single exponential decay (1, 3, 4,

Table 2. Fitting parameters for 608-nm excitation experiments

Wavelength, nm	a_1	τ_1	a_2	τ_2	a_3	τ_3
880	—	—	78 ± 3	2.56 ± 0.10	22 ± 5	8.8 ± 9.8
900	-23 ± 2	0.14 ± 0.05	58 ± 2	2.62 ± 0.12	19 ± 6	9.2 ± 12.9
920	-21 ± 1	0.19 ± 0.03	61 ± 1	2.66 ± 0.09	17 ± 3	9.8 ± 10.0
940	-20 ± 1	0.25 ± 0.05	60 ± 2	2.80 ± 0.15	19 ± 5	11.5 ± 12.5
920*	-21 ± 5	0.20 ± 0.05	59 ± 4	2.66 ± 0.20	20 ± 5	10.5 ± 13.0
920†	—	—	38 ± 5	10.0 ± 3	62 ± 8	70 ± 20

*R26 Q_A in its normal state.

†*Rb. capsulatus* mutant Tyr M208 → Thr.

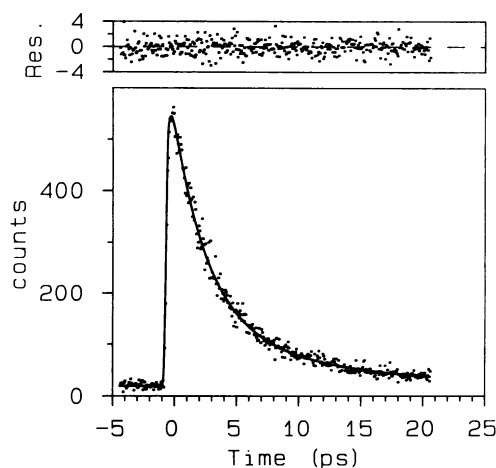


FIG. 2. Spontaneous emission decay of P* in R26 with excitation at 608 nm and emission at 920 nm. Fitting of the data (solid line) gives $a_1 = -23\%$, $\tau_1 = 0.19$ ps, $a_2 = 58\%$, $\tau_2 = 2.66$ ps, $a_3 = 17\%$, and $\tau_3 = 9.8$ ps.

9, 12, 26). However, the reported decay times for R26 have varied from 2.6 ps to 2.8 ps (9, 12) through 3.5 ps (2, 7, 8) up to 4.1 ps (26). Previous studies have been carried out at 10- to 30-Hz repetition rate, so the possibility exists that the much higher repetition rates used here [80 MHz (850 nm) and 100 kHz (608 nm)] induce the longer component. To carry out the high-repetition-rate studies, we worked with Q_A -reduced or Q_A -removed RCs. Several lines of evidence suggest that modification of Q_A does not influence the decay of P*. (i) The results in Table 1 are insensitive to the absence or reduction of Q_A , and the results in Table 2 are insensitive to whether Q_A is in its normal state or removed. (ii) Stimulated emission measurements carried out at 20-Hz repetition rate with Q_A in its normal state or reduced give indistinguishable results. The lack of a repetition-rate dependence in our fluorescence data (Tables 1 and 2) and the recent results of Vos *et al.* (5) suggest that our data are not distorted because of the high repetition rate. (iii) Hamm and Zinth^{††} have reported the observation of a 10-ps component in spontaneous emission detected in a 10-Hz-repetition-rate experiment and Holzwarth *et al.*^{‡‡} have also reported the observation of a 10-ps fluorescence decay component from time-correlated single-photon counting measurements. We conclude, then, that the nonexponentiality is intrinsic to the decay of P* in RCs. The longer component was not detected earlier in stimulated-emission measurements, presumably because of limited signal/noise ratios and lack of precise determination of the long-time signal amplitude. It seems likely that the range of P* lifetimes reported by various groups results from the different time ranges used to fit the data.

In discussing the origin of the nonexponential decay we first note that it seems likely, given the measured yield of charge separation ($\approx 100\%$) (27), but not proven, that the slow component corresponds to electron transfer with a reduced rate. We will assume that the entire decay of P* results from electron transfer in the following discussion.

Perhaps the most reasonable origin of the nonexponential decay is a distribution in the parameters influencing the electron transfer rate. It is also possible that the electron transfer process is intrinsically nonexponential as a result of the kinetic scheme (see below), slow vibrational relaxation,

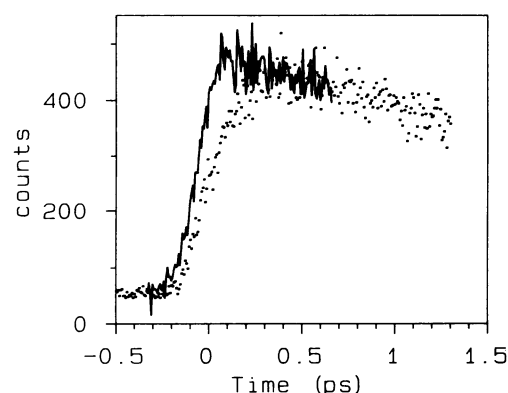


FIG. 3. Spontaneous emission decay of P* in R26 at 940-nm emission with 850-nm (solid line) and 608-nm (dots) excitation.

or protein relaxation. Chromophore and protein relaxation on the electron transfer time scale may lead to a time-dependent fluorescence spectrum, which would then give nonexponential time dependence at particular emission wavelengths. Our limited data set is not definitive on this point, but the data in Table 2 indicate that the decay kinetics vary very little across the RCs static fluorescence spectrum. This suggests that any spectral evolution is small and will not cause a large deviation from single exponential decay.

Hole-burning studies of RCs have shown the inhomogeneous distribution of P-P* energy gaps has a width of ≈ 200 cm^{-1} . This width can depend on the detergent used to isolate the RCs and the glass in which the RCs are suspended for the low-temperature hole-burning measurements (28). To explore the role of inhomogeneity, we have simulated the fluorescence of P*, assuming a purely superexchange mechanism and a Gaussian distribution in the vertical energy difference, δE , between P*BH and P*B⁻H (11). Since the superexchange coupling strength in the most naive model is proportional to $V_{PB}V_{BH}/\delta E$, this model amounts to a distribution of electronic coupling matrix elements. A distribution in site energies, without a corresponding distribution of coupling strengths, is unlikely to generate nonexponential kinetics at room temperature (G. Small, personal communication). In Fig. 4 *Upper* the distribution in δE is narrow with respect to the mean value of δE and the decay is exponential. However, when the distribution is broad compared to the mean value of δE , the superexchange mechanism gives rise to nonexponential behavior (Fig. 4 *Lower*). While this is a

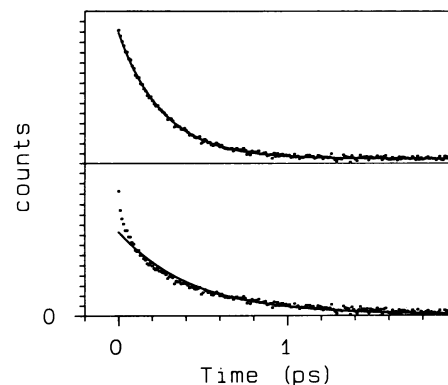


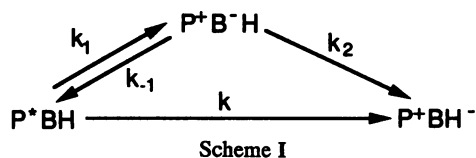
FIG. 4. Simulation of P* decay with superexchange mechanism considering a Gaussian distribution of energy gaps (δE) between P*B⁻H and P*BH. (*Upper*) Calculation with $\delta E = 1600 \pm 300$ cm^{-1} (solid line) and single exponential decay with $\tau_1 = 2.6$ ps (dotted line). (*Lower*) $\delta E = 500 \pm 300$ cm^{-1} (solid line) and single exponential decay with $\tau_1 = 2.6$ ps (dotted line).

^{††}P. Hamm & W. Zinth, Ultrafast Phenomena VIII. Antibes-Juan-les-Pines, France, June 8–12, 1992 (abstr. TuC29).

^{‡‡}M. G. Muller, K. Griebenow & A. R. Holzwarth, Ultrafast Phenomena VIII. Antibes-Juan-les-Pines, France, June 8–12, 1992 (abstr. TuC22).

simplified example, it serves to illustrate that a distribution in one parameter affecting the electron transfer rate can give rise to nonexponential behavior. The strongest evidence supporting the argument for inhomogeneity is that for the series of mutants we have measured the width of the P₊-absorption band of the dimer appears to increase as the amplitude of the long time component in the fluorescence decay increases. For the Tyr M208 → Phe mutant (46.7% long time component) the full width at half-maximum at 4 K is $\approx 642\text{ cm}^{-1}$ while for the Phe L181 → Tyr mutant (15.6% long time component) it is $\approx 561\text{ cm}^{-1}$. However, the width of the absorption band may also change as a result of alteration of the frequency or displacement (S) of the mode strongly coupled to the optical transition (28).

A second, but not exclusive, possibility is that the system is homogeneous and the kinetic scheme for the decay of P* gives intrinsically nonexponential decay. To investigate this we consider the parallel sequential superexchange scheme.



We neglect the reverse rates for the superexchange process (k) and for the second step in the sequential process because of the large energy gaps involved. The solution to this scheme has been given (11). In the following analysis we assume that thermal equilibrium is established rapidly and therefore $k_{-1} = k_1 \exp(-\Delta G_1/k_B T)$, where ΔG_1 is the (free) energy gap between P*BH and P*B-H. In the following discussion we consider the case where Scheme I alone is responsible for the nonexponential decays. Fig. 5 shows a plot of all values of the four rate constants that give a P* decay of 2.7 ps (72.3%) and 11.1 ps (27.7%) as a function of ΔG_1 . (A negative value of ΔG_1 means that P*B-H is lower in energy than P*BH.) The first conclusion from Fig. 5 is that values of ΔG_1 can only be in the range $-350\text{ cm}^{-1} \leq \Delta G_1 \leq 120\text{ cm}^{-1}$. Values outside this range do not yield meaningful physical solutions. Values of ΔG_1 in this range give a sizable transient concentration of P*B-H. (The maximum concentration of P*B-H ranges from $\approx 46\%$ at $\Delta G_1 = -350\text{ cm}^{-1}$ to 12% at $\Delta G_1 = 120\text{ cm}^{-1}$ of the initial concentration of P*.) The large concentrations of P*B-H do not appear consistent with transient-absorption studies (1–4, 7, 8, 12). When we restrict the maximum concentration of P*B-H to be $< 20\%$ of the initial concentration of P*, and if the kinetic Scheme I is the sole origin of the biexponential decay, this would imply that $-100\text{ cm}^{-1} \leq \Delta G_1 \leq 150\text{ cm}^{-1}$, which is in agreement with our analysis for transient absorption (6). The second conclusion is that the rate constant for the second step, k_2 , is always smaller than the forward rate constant of the first step. This is the reverse of the usual assumptions (1, 3–5, 10, 11). However, the reverse rate constant, k_{-1} , is also competing with the forward

rate constant, k_1 , to delete the population of the state P*B-H (Scheme I). We should compare the sum of k_{-1} and k_2 with k_1 . The sum of k_{-1} and k_2 may be larger than k_1 (Fig. 5). The third conclusion is that the transient concentration of P*B-H is not zero even when the reaction proceeds only via the superexchange mechanism. The reason is that the sequential mechanism can be blocked at the second step while the first step is still active. From a different approach, where a simple three-state model is used, Joseph *et al.* (13) have discussed the contribution to the intermediate-state population from the superexchange mechanism. Those authors concluded that in the superexchange process, there should be some population in the intermediate state, even though it may be small.

A similar analysis was carried out for *Rb. capsulatus* and the four mutants. The acceptable ranges of ΔG_1 are -350 to $+120\text{ cm}^{-1}$ (wild type), -460 to $+70\text{ cm}^{-1}$ (Phe L181 → Tyr), -180 to $+60\text{ cm}^{-1}$ (Phe L181 → Tyr, Tyr M208 → Phe), -160 to $+80\text{ cm}^{-1}$ (Tyr M208 → Phe), and -50 to 240 cm^{-1} (Tyr M208 → Thr). The oxidation potential of P has been measured chemically for a large set of *Rb. capsulatus* mutants including all those listed in Table 1. The full data set will be discussed in detail elsewhere (J.R.N., T.J.D., and M. Popov, unpublished work), but the trends from the kinetic model and the chemical measurements seem similar, implying that the kinetic scheme may contribute to the observed nonexponential decays. We emphasize that in all cases $k_2 < k_1$, and if this can be shown to be incompatible with experimental data, explanation of the nonexponentiality based on parallel (and reversible) paths in a homogeneous system can be rejected.

In several publications Zinth and coworkers (2, 7, 8) have discussed the primary charge separation step in terms of two consecutive, irreversible steps. They assign a 3.5-ps time constant to the first step and a 0.9-ps time constant to the second. Their analysis clearly invalidates the model described above; however, two other groups differ in their interpretation of their own and Zinth and coworkers' data. Vos *et al.* (5) state that a linear two-step sequential model is inconsistent with their data, while Holten and Kirmaier (3, 4) suggest that a distribution of RCs with differing electron transfer rates complicates the interpretation provided by Zinth and coworkers. Holten and Kirmaier suggest that their data appear more readily reconcilable with a single-step superexchange mechanism. In a recent publication from our laboratory the bleaching kinetics of the active-branch pheophytin (H_A) were analyzed in the context of a reversible two-step process, a single-step mechanism, or a combination of the two (9). By comparing the bleaching kinetics with the decay of stimulated emission from P* it was concluded that the two-step mechanism was appropriate at room temperature. Clearly this conclusion needs to be reexamined in the light of the more complex decay of P* observed in this work. A full discussion of this reanalysis will be given elsewhere. For the present we simply note the major discrepancy between the P* decay and the bleaching observed at 545 nm for the R26 sample is the slower rise of the bleaching in the 0- to 5-ps region as compared with the P* decay (9). The presence of a slow component of $\approx 20\%$ amplitude in the P* decay does not appreciably influence this portion of the bleaching kinetics, and thus the new data do not remove this discrepancy. They do, however, complicate the analysis given in ref. 9, and higher signal/noise bleaching data are necessary to address this issue further.

The third alternative that we wish to consider is that of slow or incomplete vibrational relaxation (29–31). An explicit quantum mechanical treatment was presented by Jean *et al.* (29, 30). In this work a numerical simulation shows nonexponential decay of the initial-state population and explores how the rate of electron transfer is complicated by the competition between the intrinsic electron transfer process and the vibrational dephasing. In a semiclassical model (Z.

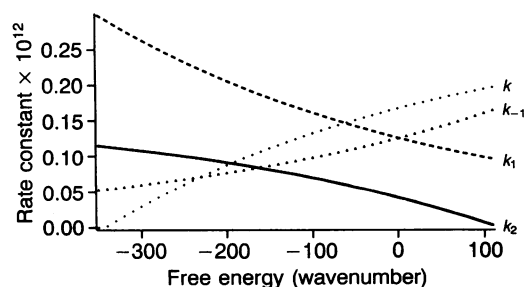


FIG. 5. Calculated rate constants as a function of free energy ΔG_1 according to the kinetic Scheme I for *Rb. capsulatus* wild type.

Wang, J. Tang, and J.R.N., unpublished work), nonexponentiality of the initial-state population decay is obtained in a numerical simulation of the RCs. A wide variety of experimental evidence is now emerging which shows that vibrational relaxation and dephasing of many high-frequency modes in large molecules is not necessarily fast compared with the time scale of photosynthetic electron transfer (M.D., Y. Jia, and G.R.F., unpublished work; ref. 32). Direct measurements of these time scales in photosynthetic systems are needed to test this hypothesis.

Finally, we briefly discuss the rise time that appeared in 608-nm experiments. As shown in the spectroscopic studies (refs. 33 and 34 and references therein), the 608-nm excitation pulse lies in the region of the Q_x band of bacteriochlorophyll, centered at ≈ 595 nm. The extensive interaction of six chromophores in RCs makes the assignment of the individual contributions of each chromophore difficult. Linear dichroism measurements (35) of *Rhodospseudomonas viridis* showed that the Q_x band of the dimer, centered at 610 nm, is red-shifted ≈ 200 cm^{-1} from the Q_x band of the accessory monomer, centered at 605 nm. Since the Q_x band does not depend significantly on the structure of the RC (33) we assume that the Q_x band of the dimer red shifts by a similar amount to the accessory monomer. In this case excitation with a pulse centered at 608 nm preferentially excites the Q_x band of the dimer and only a small fraction of the accessory chlorophyll is excited.

A possible origin of the rise time may be (i) energy transfer from accessory monomer to the special pair and/or internal conversion of the special pair from Q_x to Q_y , (ii) coherent effects in the preparation and detection processes (13–15, 29, 30, 35), and (iii) protein and/or medium relaxation (11). Mechanisms ii and iii do not seem consistent with our inability to resolve rise time in the 850-nm experiments. However, the excitation pulse durations were different in the two experiments [≈ 49 fs for 608 nm ($\Delta\nu \approx 300$ cm^{-1}) and ≈ 113 fs ($\Delta\nu \approx 130$ cm^{-1}) for 850 nm]. Therefore, the initial state may have a different character in the two cases (for example, the 49 fs is impulsive with respect to the 100 cm^{-1} mode whereas the 113-fs pulse effectively is not). Further investigation is needed to explore these mechanisms. However, we can conclude the excitation becomes located in the lower state of the special pair extremely rapidly, and the electron transfer process follows a similar or the same route independent of the initial state prepared.

CONCLUSION

We have measured the spontaneous emission from P^* in R26, *Rb. capsulatus*, and mutants of *Rb. capsulatus* with 50-fs time resolution. In all RCs the fluorescence decay can be well fit as a double exponential. The short time constant obtained from these fits agrees well with previous stimulated-emission results (9). We propose three mechanisms that may give rise to the nonexponential decay: (i) a distribution in parameters influencing the electron transfer rate, (ii) a homogeneous system and a combination of rate constants for a two-step and superexchange kinetic scheme that yields nonexponentiality, and (iii) slow or incomplete vibrational relaxation on the electron transfer time scale.

At present the most likely explanation for our nonexponential decay of the spontaneous (and stimulated) emission from bacterial RCs seems to be that a distribution of intrinsic electron transfer rates exists within an ensemble of RCs. A quantitative analysis of this effect must await more detailed analysis of the low-temperature spectra.

We thank M. Armas, C. Seaton, and A. Swygard of Coherent for the loan of the Mira laser. We thank Dr. C.-K. Chan for many helpful discussions, and G. Small for providing us with low-temperature absorption spectra. We thank N. Scherer for development of the dye laser used in this experiment. This work was supported by a grant from the National Science Foundation (G.R.F.), by the Department of Energy, Office of Basic Energy Sciences (J.R.N.) and Office of Health and Environmental Research (D.K.H. and M.S.) under Contract W-31-109-Eng-38. M.S. is also supported by U.S. Public Health Service Grant GM36598. This work is a publication of the Center for Photochemistry and Photobiology.

- Holten, D. & Kirmaier, C. (1987) *Photosynth. Res.* **13**, 225–260.
- Lauterwasser, C., Finklele, U., Scheer, H. & Zinth, W. (1991) *Chem. Phys. Lett.* **183**, 471–477.
- Holten, D. & Kirmaier, C. (1990) *Proc. Natl. Acad. Sci. USA* **87**, 3552–3556.
- Holten, D. & Kirmaier, C. (1991) *Biochemistry* **30**, 609–613.
- Vos, M. H., Lambry, J.-C., Robles, S. J., Youvan, D. C., Breton, J. & Martin, J.-L. (1991) *Proc. Natl. Acad. Sci. USA* **88**, 8885–8889.
- Vos, M. H., Lambry, J.-C., Robles, S. J., Youvan, D. C., Breton, J. & Martin, J.-L. (1992) *Proc. Natl. Acad. Sci. USA* **89**, 613–617.
- Holzappel, W., Finklele, U., Kaiser, W., Oesterheld, D., Scheer, H., Stolz, H. U. & Zinth, W. (1990) *Proc. Natl. Acad. Sci. USA* **87**, 5168–5172.
- Holzappel, W., Finklele, U., Kaiser, W., Oesterheld, D., Scheer, H., Stolz, H. U. & Zinth, W. (1989) *Chem. Phys. Lett.* **161**, 1–7.
- Chan, C.-K., DiMaggio, T. J., Chen, L. X.-Q., Norris, J. R. & Fleming, G. R. (1991) *Proc. Natl. Acad. Sci. USA* **88**, 11202–11207.
- Hu, Y. & Mukamel, S. (1989) *J. Chem. Phys.* **91**, 6973–6988.
- Bixon, M., Jortner, J. & Michel-Beyerle, M. E. (1991) *Biochim. Biophys. Acta* **1056**, 301–312.
- Fleming, G. R., Martin, J. L. & Breton, J. (1988) *Nature (London)* **333**, 190–192.
- Joseph, J. S., Bruno, W. & Bialek, W. (1991) *J. Phys. Chem.* **95**, 6242–6247.
- Marcus, R. A. & Almeida, A. (1990) *J. Phys. Chem.* **94**, 2973–2977.
- Almeida, A. & Marcus, R. A. (1990) *J. Phys. Chem.* **94**, 2978–2989.
- Wright, C. A. (1979) *Biochem. Biophys. Acta* **548**, 309–313.
- DiMaggio, T. J. (1991) Ph.D. thesis (The University of Chicago).
- Woodbury, N. W. T., Parson, W. W., Gunner, M. R., Prince, R. C. & Dutton, P. L. (1986) *Biochim. Biophys. Acta* **851**, 6–22.
- Okaamura, M. Y., Isaacson, R. A. & Feher, G. (1985) *Biophys. J.* **48**, 849–857.
- Ruggiero, A. R., Scherer, N. F., Mitchell, C. M., Fleming, G. R. & Hogan, J. N. (1991) *J. Opt. Soc. Am. B Opt. Phys.* **8**, 2063–2067.
- Xie, X., Du, M., Mets, L. & Fleming, G. R. (1992) *Proceedings of the International Society for Optical Engineering OE/LASE (SPIE, Bellingham, WA)*, p. 1640.
- Pearson, E. S. & Hartley, H. O., eds. (1976) *Biometrika Tables for Statisticians* (Biometrika Trust, London), Vol. 1.
- Rosenthal, S. J. (1992) Ph.D. thesis (The University of Chicago).
- Chan, C.-K., Chen, L. X.-Q., DiMaggio, T. J., Hanson, D. K., Nance, S. L., Schiffer, M., Norris, J. R. & Fleming, G. R. (1991) *Chem. Phys. Lett.* **176**, 366–372.
- Shah, J. (1988) *IEEE J. Quantum Electron.* **24**, 276–288.
- Woodbury, N. W., Becker, M., Middendorf, D. & Parson, W. W. (1985) *Biochemistry* **24**, 7516–7521.
- Parson, W., Clayton, R. K. & Cogdell, C. J. (1975) *Biochim. Biophys. Acta* **387**, 265–278.
- Johnson, S. G., Tang, D., Jankowiak, R., Hayes, J. M., Small, G. J. & Tiede, D. M. (1990) *J. Phys. Chem.* **94**, 5849–5855.
- Jean, J., Friesner, R. A. & Fleming, G. R. (1991) *Ber. Bunsenges. Phys. Chem.* **95**, 253–257.
- Jean, J., Friesner, R. A. & Fleming, G. R. (1992) *J. Chem. Phys.* **96**, 5827–5842.
- Bixon, M. & Jortner, J. (1982) *Faraday Discuss. Chem. Soc.* **74**, 17–29.
- Dexheimer, S. L., Wang, Q., Peteanu, L. A., Pollard, W. T., Mathies, R. A. & Shank, C. V. (1992) *Chem. Phys. Lett.* **188**, 61–66.
- Pearlstein, R. M. (1982) in *Photosynthesis: Energy Conversion by Plants and Bacteria*, ed. Govindjee (Academic, New York), Vol. 1, p. 293.
- Knapp, E. W., Fischer, S. F., Zinth, W., Sander, M., Kaiser, W., Deisenhofer, J. & Michel, H. (1985) *Proc. Natl. Acad. Sci. USA* **82**, 8463–8467.
- Loring, R. F., Yan, Y. J. & Mukamel, S. (1987) *J. Chem. Phys.* **87**, 5840–5857.